Chiral nematic liquid crystals in cylindrical cavities

M. Ambrožič[1] and S. Žumer[1,2]
[1]*J. Stefan Institute, University of Ljubljana, Jamova 39, Ljubljana, Slovenia*
[2]*Physics Department, University of Ljubljana, Jadranska 19, Ljubljana, Slovenia*
(Received 4 June 1996)

We report a theoretical study of various structures of chiral nematic liquid crystals, confined to submicrometer cylindrical cavities with tangential anchoring conditions. The Frank-Oseen free energy with additional surface energy terms is used to find nematic director fields, free energies, and stability diagrams of relevant structures. The dependence of various chiral nematic structures on the chirality parameter, pore size, elastic constants, and polar and azimuthal surface anchoring strengths is studied. We are particularly interested in the influence of the saddle-splay elastic constant on the structures. For ordinary values of material parameters, only radially twisted and asymmetric conical structure are stable. The former is stable at low chiralities, while the latter is stable for high chiralities. The radially twisted structure is commonly known as double twisted structure, while the asymmetric conical structure has not been considered, to the authors' knowledge. The phase diagram including both structures is determined by comparing their free energies. Theoretical predictions are in agreement with available experimental data. [S1063-651X(96)01811-9]

PACS number(s): 61.30.Cz, 64.70.Md, 61.30.Jf, 68.10.Cr

I. INTRODUCTION

Chiral nematic liquid crystals attract interest for fundamental and practical reasons [1,2]. Since the discovery of polymer dispersed liquid crystals numerous experimental and theoretical works have been performed on liquid crystals confined to spherical and cylindrical geometries. Membranes with well-defined submicrometer cylindrical pores allow for detailed studies of highly curved confinement [3,4]. Cavity walls may be chemically treated to achieve the desired anchoring conditions. The behavior of chiral nematics in the curved confining geometry was reported by Cladis, White, and Brinkman [5]. Using optical polarizing microscopy, they studied chiral nematic structures in supramicrometer capillary tubes with homeotropic anchoring near the transition to the smectic-*A* phase. Lequeux and Kleman [6] observed a helicoidal instability of the double-twisted structure (observed also in blue phases and here more precisely called the radially twisted structure) in capillary tubes with homeotropic anchoring by polarizing microscope. Bezič and Žumer studied defects of chiral nematic model structures in spherical and cylindrical confining geometry [7,8]. NMR is a useful tool for investigations of nematic structures in submicrometer pores, where the optical microscopy is too rough [9–11]. Using deuterium NMR spectroscopy, Ondris-Crawford *et al.* [10] studied a pitch-induced transition of chiral nematic liquid crystals in submicrometer cylindrical cavities in Anopore membranes.

We study defectless chiral nematic liquid-crystal structures in cylindrical cavities with radii small compared to the cylinder lengths, so that end effects can be neglected. We investigate two kinds of planar anchoring conditions: degenerate planar anchoring and anchoring with the preferred direction parallel to the cylinder axis (abbreviated *z* anchoring). We calculate nematic director fields, free energies, and stability ranges of radially twisted structures and other model structures, with twist axes parallel or perpendicular to the cylinder axis.

In Sec. II we establish theoretical grounds for our phenomenological description of structures. In Sec. III we discuss relevant solutions of the Euler-Lagrange equations for various model structures. We also compare the corresponding free energies and calculate the stability phase diagrams. In Sec. IV we analyze some available experimental results and estimate values of both anchoring strengths and the saddle-splay elastic constant. In Sec. V we discuss results and give a conclusion.

II. FREE ENERGY

Our chiral nematic liquid crystal is simply described by a nematic director field $\vec{n}(\vec{r})$ with an equivalence of $\vec{n}$ to $-\vec{n}$. We neglect the biaxiality and space variation of the scalar nematic order parameter. Polar coordinates r, ϕ, and z are used for the calculation of the director fields and corresponding free energies in cylindrical geometry, where z is in the direction of the cylinder axis. We denote the polar orthonormal set of vectors by $\vec{e}_r$, $\vec{e}_\phi$, and $\vec{e}_z$. The free energy of a chiral nematic liquid crystal in a cavity is usually divided into a bulk and a surface term

$$F=\int f_V dV+\int f_S dS. \tag{1}$$

The bulk Frank-Oseen free-energy density [12] is a sum of elastic deformation energy terms with different symmetries

$$f_V=\tfrac{1}{2}[K_{11}(\vec{\nabla}\cdot\vec{n})^2+K_{22}(\vec{n}\cdot\vec{\nabla}\times\vec{n}+q)^2+K_{33}(\vec{n}\times\vec{\nabla}\times\vec{n})^2 - K_{24}\vec{\nabla}\cdot(\vec{n}\times\vec{\nabla}\times\vec{n}+\vec{n}\vec{\nabla}\cdot\vec{n})], \tag{2}$$

where K_{11}, K_{22}, and K_{33} are splay, twist, and bend elastic constants, respectively, and K_{24} is the saddle-splay elastic constant. To make our discussion as simple as possible we omitted the K_{13} (splay-bend) energy term. The positive chirality parameter q corresponding to the right-handed helix is inversely proportional to the pitch of the unconfined phase:

$q=2\pi/p$. We call it the ''natural inverse pitch'' to distinguish it from the ''actual inverse pitch'' q' in the confined geometry.

In the case of homogeneous planar anchoring the surface free-energy density in the Rapini-Papoular approximation [13] is the sum of a polar (out-of-plane) and an azimuthal (in-plane) surface elastic term. For the description of experimentally studied Anopore membranes, nondegenerate planar anchoring with the easy axis parallel to the cylinder axis (z axis) is assumed. This anchoring direction is probably effectively enforced by slightly nonspherical cross sections of cylindrical cavities. Thus one can write

$$f_S=\tfrac{1}{2}(W_\phi\sin^2\phi'+W_\theta\cos^2\phi')\sin^2\theta', \tag{3}$$

where W_ϕ and W_θ are the azimuthal and the polar anchoring strength, respectively, θ' is the angle between the nematic director and the z axis, and ϕ' is the angle between the $(\vec{n},\vec{e}_z)$ plane and the $(\vec{e}_r,\vec{e}_z)$ plane. In the case of degenerate planar anchoring W_ϕ is zero and the surface free-energy density reduces to $f_S=\frac{1}{2}W_\theta\sin^2\theta$, where θ is the angle between the nematic director and its projection on the boundary plane. We focus our attention on the approximation of equal splay and bend elastic constants $K_{11}=K_{33}$. This yields a simple free energy and the corresponding Euler-Lagrange equations. Nevertheless, the solutions have all the relevant features of more general ones. Furthermore, we limit ourselves to cylinder radii R small compared to lengths l. To avoid a strange kind of anchoring, where the preferable plane would be $(\vec{e}_\rho,\vec{e}_z)$ instead of $(\vec{e}_\phi,\vec{e}_z)$, we take into account the condition $W_\phi\leqslant W_\theta$. It is convenient to introduce dimensionless (''reduced'') quantities for the radius vector, chiralities, elastic constants, and anchoring strengths:

$$\rho=\frac{r}{R}, \tag{4}$$

$$\mathcal{Q}=qR, \tag{5}$$

$$\mathcal{Q}'=q'R, \tag{6}$$

$$\mathcal{K}_{22}=K_{22}/K_{33}, \tag{7}$$

$$\mathcal{K}_{24}=K_{24}/K_{33}, \tag{8}$$

$$\mathcal{W}_\phi=RW_\phi/K_{33}, \tag{9}$$

$$\mathcal{W}_\theta=RW_\theta/K_{33}, \tag{10}$$

$$\mathcal{F}=\frac{F}{K_{33}\pi l}, \tag{11}$$

$$\mathcal{W}_+=\mathcal{W}_\theta+\mathcal{W}_\phi, \tag{12}$$

$$\mathcal{W}_-=\mathcal{W}_\theta-\mathcal{W}_\phi. \tag{13}$$

In the following section we describe chiral nematic structures that were considered in our search for the most stable chiral ordering.

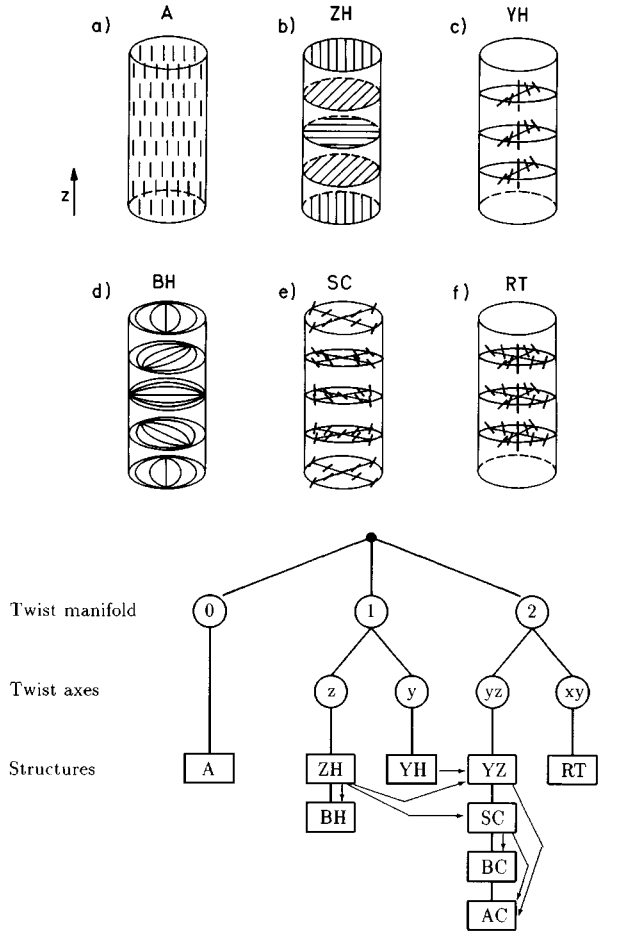

FIG. 1. Upper part: simple chiral nematic structures in cylinder cavities: (a) axial (A), (b) z helical (ZH), (c) y helical (YH), (d) bipolar helical (BH), (e) simple conical (SC), and (f) radially twisted (RT). An arrow indicates the direction of the z axis. Bottom: grouping of all discussed [including yz twisted (YZ), bipolar conical (BC), and asymmetric conical (AC)] structures according to their twist character. Arrows indicate the generalization of one structure into another.

III. MODEL CHIRAL NEMATIC STRUCTURES IN CYLINDERS

A straightforward search for general structures in cylindrical cavities with planar anchoring would be a big numerical task. Therefore, we instead choose various model structures and check for their thermodynamic stability. According to the twist character, we can divide them into three main groups. In the first group there is only the axial (A) structure with no twist. In the second group there are structures with a twist around a single axis. Furthermore, we can divide this group into two subgroups, where the chosen twist axis is z (along the cylinder axis) or y (perpendicular to the cylinder axis), respectively. In the first subgroup there are z helical (ZH) structure and bipolar helical (BH) structure, while in the second subgroup we have y helical (YH) structure. The third group, which contains structures with a twist around two axes, can also be divided into two subgroups. In the first one, where the local twist axes are y and z, there is a yz twisted (YZ) structure and three kinds of conical structures: simple (SC), bipolar (BC), and asymmetric (AC). In the sec-

ond subgroup with twist axes x and y there is only radially twisted (RT) structure. In Fig. 1 the majority of these structures are schematically presented; also the twist character and connections between different structures are shown. The number and directions of local twist axes need not be seen immediately, but one can determine them by using the twist pseudotensor introduced by Kilian and Sonnet [14].

A. Axial structure

In this structure the nematic director is parallel to the cylinder axis: $\vec{n}=\vec{e}_z$. Its free energy originates from the twist elastic term $\mathcal{F}=\frac{1}{2}\mathcal{Q}^2$. The axial structure is stable only in the limit of zero chirality.

B. z helical structure

This structure corresponds to the helical structure of unconfined chiral nematic liquid crystals, with the helical axis parallel to cylinder axis: $\vec{n}=(\cos qz,\sin qz,0)$. Its free energy is equal to $\frac{1}{2}\mathcal{W}_+$.

C. Bipolar helical structure

This structure is a generalization of a planar bipolar structure [9], which is characteristic for nonchiral nematic liquid crystals, confined to cylinders with concentric planar anchoring. The director field of a bipolar helical structure can be written as $\vec{n}=\cos\psi(\rho,\phi')\vec{e}_r+\sin\psi(\rho,\phi')\vec{e}_\phi$, where ψ is the angle between the radius unit vector $\vec{e}_r$ and the local nematic director. The rotation of the symmetry axis x around the z axis is incorporated in the linear increase of the polar angle yielding the polar angle in a rotating coordinate system $\phi'=\phi-q'z$. The actual chiral parameter q' can be different from the natural one (q). Since the BH structure has already been reported (see the axially twisted planar bipolar structure in Ref. [10]), only a short description will be given here. The twist elastic constant can be integrated into the inverse pitch $\mathcal{Q}\to\sqrt{\mathcal{K}_{22}}\mathcal{Q}$ or $\mathcal{Q}'\to\sqrt{\mathcal{K}_{22}}\mathcal{Q}'$. So it is sufficient to describe the $\mathcal{K}_{22}=1$ results. The K_{24} energy term is zero in this structure. The minimization of the Frank free energy results in a partial differential equation for the angle ψ, which is solved numerically. Finally, the actual inverse pitch q' is adjusted to give the lowest free energy. The nematic director does not depend on the azimuthal and polar anchoring strengths separately, but only on their difference $\mathcal{W}_-$. The free energy can be written as a sum of a part, which corresponds to degenerate planar anchoring, and an azimuthal anchoring strength $\mathcal{F}(\mathcal{W}_\phi,\mathcal{W}_\theta,\mathcal{Q},\dots)=\mathcal{F}(0,\mathcal{W}_-,\mathcal{Q},\dots)+\mathcal{W}_\phi$. In the case of equal anchoring strengths $\mathcal{W}_\phi=\mathcal{W}_\theta=\frac{1}{2}\mathcal{W}_+$ this reduces to the z helical value $\frac{1}{2}\mathcal{W}_+$.

In the limit of zero chirality the solution converges to the ordinary planar bipolar structure [9] for nonchiral nematic liquid crystals:

$$\psi(\rho,\phi)=-\arctan\left(\tan\phi\,\frac{1+\gamma\rho^2}{1-\gamma\rho^2}\right), \tag{14}$$

where $\gamma=\sqrt{\xi^2+1}-\xi$ and $\xi=2/\mathcal{W}_\theta$. For small chiralities $\mathcal{Q}<0.5$ the use of Eq. (14) is justified, except ϕ must be substituted by ϕ'. The shape of the nematic director field in the ''helical'' (x,y) plane is nearly the same as for zero chirality, except that the symmetry x axis rotates around the z axis. For higher chiralities the director field in the helical plane is better aligned (Fig. 2) and in the high-chirality limit we obtain a z helical structure. The actual chirality $\mathcal{Q}'$ is somewhat smaller than the natural value $\mathcal{Q}$. The difference $\mathcal{Q}-\mathcal{Q}'$ is smaller than 0.2 in the whole range ($0<\mathcal{Q}<\infty$ and $0<\mathcal{W}_\theta<5$) that we studied. The difference is the largest for chiralities of order 1. In the zero- and high-chirality limit the difference between chiralities vanishes.

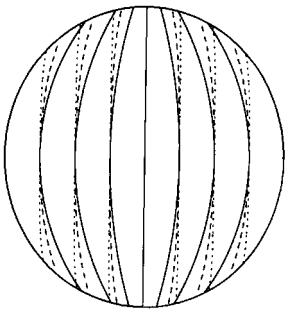

FIG. 2. Nematic director field of the BH structure for $\mathcal{K}_{22}=1$, $\mathcal{W}_-=4$, and three different values of chirality: $\mathcal{Q}=0$ (solid lines), $\mathcal{Q}=2$ (dashed lines), and $\mathcal{Q}=5$ (dotted lines).

For fixed values of other physical parameters the calculated free energy increases with chirality. In the high-chirality limit the free energy approaches the helical value $\mathcal{W}_+/2$.

D. y helical structure

y helical structure is similar to z helical structure, except that here we have a twist of nematic director around the y axis rather than around the z axis. To avoid a repetition, we will describe the behavior of the free energy together with the results for a more general yz twisted structure. Here we just mention the somehow surprising result that the YH free energy has been found to be always lower than the ZH and BH free energies.

E. yz twisted structure

In the yz twisted structure there is a twist of the nematic director around two axes: the z cylinder axis and an axis, perpendicular to z, say, the y axis. The nematic director can be written as

$$\vec{n}=(\cos(q'z)\sin\beta,\sin(q'z)\sin\beta,\cos\beta), \tag{15}$$

where $\beta=q''y'+\alpha$ and $y'=-x\sin(q'z)+y\cos(q'z)$. Here β is the angle of the rotation of the nematic director around the local y' axis with inverse pitch q'', while the axis y' rotates around the z axis with inverse pitch q'. If there was no rotation around the z axis, the nematic director would be $\vec{n}=(\sin\beta,0,\cos\beta)$ with $\beta=q''y+\alpha$. In this case one would have a y helical structure. With the additional rotation around the z axis, both nematic director components and Cartesian variables must be transformed. On the other hand, the z helical structure is also a special case of the yz twisted structure. We have added an optional angle α to the twist angle β, which influences the free energy. Similarly, we could add an angle to the twist angle $q'z$ around the z axis, but this would have no effect on the free energy because we

assume long cylinders and periodicity in the z direction. First the free energy is calculated and then the free parameters q', q'', and α are adjusted to minimize it. In confined systems, both chiralities q' and q'' are generally different from the natural chirality q. The nematic director can be easily transformed into cylindrical coordinates

$$\vec{n}=\sin\beta\,\cos\phi'\vec{e}_\rho-\sin\beta\,\sin\phi'\vec{e}_\phi+\cos\beta\vec{e}_z,$$

where, as for the BH structure, $\phi'=\phi-q'z$ is the azimuthal angle in the coordinate system rotating around the z axis. To make equations simpler, we calculated the bulk and surface free-energy densities only in the case of equal elastic constants:

$$f_V=\frac{K}{2R^2}\,[(Q''-Q)^2+(2(1-\mathcal{K}_{24})\mathcal{Q}'\mathcal{Q}''-2\mathcal{Q}\mathcal{Q}'+\mathcal{Q}'^2)\sin^2\beta+(\mathcal{Q}'\mathcal{Q}''\rho\,\cos\phi')^2], \quad (16)$$

$$f_S=\frac{K}{2R}\,(\mathcal{W}_\phi\sin^2\phi+\mathcal{W}_\theta\cos^2\phi)\sin^2\beta. \quad (17)$$

Of course, here we take $\mathcal{Q}=qR$, and similarly for $\mathcal{Q}'$ and $\mathcal{Q}''$. According to the relation for the Bessel functions $J_n(x)=(1/2\pi)\int_0^{2\pi}\cos(x\,\sin\phi-n\phi)d\phi$, the resulting dimensionless free energy is

$$\mathcal{F}=\frac{1}{2}\,(\mathcal{Q}''-\mathcal{Q})^2+\frac{\mathcal{Q}'}{4}\,[2(1-\mathcal{K}_{24})\mathcal{Q}''-2\mathcal{Q}+\mathcal{Q}']\times\left(1-\cos(2\alpha)\,\frac{J_1(2\mathcal{Q}'')}{\mathcal{Q}''}\right)+\frac{1}{8}\,(\mathcal{Q}'\mathcal{Q}'')^2+\frac{1}{4}\times\{\mathcal{W}_+[1-\cos(2\alpha)J_0(2\mathcal{Q})]-\mathcal{W}_-\cos(2\alpha)J_2(2\mathcal{Q})\}. \quad (18)$$

The angle α can be either 0 or $\pi/2$: this corresponds to the nematic director at the cylinder axis parallel or normal to the axis, respectively. The optimal value of the chirality around the z axis $\mathcal{Q}'$ can be expressed in terms of $\mathcal{Q}''$. The optimal value of $\mathcal{Q}''$ is obtained numerically. Keeping anchoring strengths and $\mathcal{K}_{24}$ fixed while increasing the natural chirality $\mathcal{Q}$, there are alternating intervals, where $\alpha=0$ or $\pi/2$. At the transition points $\alpha=0\leftrightarrow\alpha=\pi/2$ there are also discontinuous jumps in $\mathcal{Q}'$, $\mathcal{Q}''$, and the slope of energy as functions of natural chirality. The $\mathcal{K}_{24}$ elastic energy term lowers the total free energy, but otherwise it does not have a significant effect on the nematic structure. In Fig. 3 the dependence of both actual chiralities on the natural chirality is shown for a particular choice of anchoring strengths. We have found that for all anchoring strengths between 1 and 10 and for natural chiralities from 0 to 30 the twist around the z axis is negligible in comparison to the twist around the y axis. $\mathcal{Q}'$ and $\mathcal{Q}''$ are comparable for low chiralities, but for the effective twisting about the z axis only the very small projection of the nematic director on the xy plane counts. The graph for all examined anchoring strengths is qualitatively the same as in Fig. 3. The zero-chirality limit of the yz twisted structure is the axial structure, while the high-chirality limit is the y helical structure (with $\mathcal{Q}''\rightarrow\mathcal{Q}$) and the limiting free energy is $\frac{1}{4}\mathcal{W}_+$, equal to half of the z helical value.

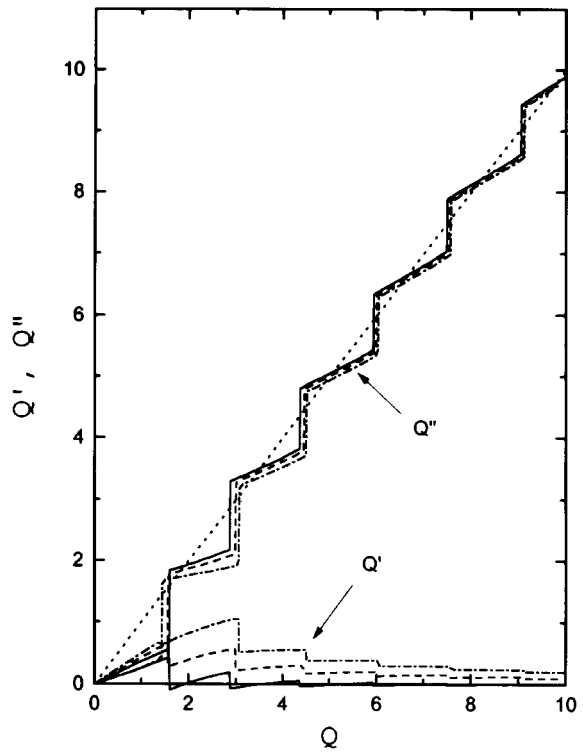

FIG. 3. Actual inverse pitches of YZ structure as functions of natural chirality for $\mathcal{K}_{22}=1$, $\mathcal{W}_\phi=\mathcal{W}_\theta=3$, and different values of saddle-splay elastic constant: $\mathcal{K}_{24}=0$ (solid lines), $\mathcal{K}_{24}=0.5$ (dashed lines), and $\mathcal{K}_{24}=1$ (dash-dotted lines). The dotted line indicates the limit $\mathcal{Q}''=\mathcal{Q}$. All chiralities are dimensionless.

F. Simple conical structure

This structure is also a generalization of the z helical structure, which was suggested by Schmiedel *et al.* on the basis of their NMR and optical experiments [15]. A deflection of the nematic director field out of the xy plane is allowed, but its projection to that plane is assumed to be in one direction: $\vec{n}=\sin\theta(\rho)\cos(q'z)\vec{e}_x+\sin\theta(\rho)\sin(q'z)\vec{e}_y+\cos\theta(\rho)\vec{e}_z$, where the tilt angle θ depends only on the radius ρ. The nematic director, rewritten in polar coordinates, is equal to $\vec{n}=\sin\theta(\rho)\cos\phi'\vec{e}_\rho-\sin\theta(\rho)\sin\phi'\vec{e}_\phi+\cos\theta(\rho)\vec{e}_z$, where, as in the BH case, we introduce the azimuthal angle $\phi'=\phi-q'z$ in the rotating coordinate system.

After integration over ϕ and z the expression for the reduced free energy becomes

$$\mathcal{F}=\int_0^1\left[\frac{1+\mathcal{K}_{22}}{2}\left(\frac{d\theta}{d\rho}\right)^2-(2\mathcal{K}_{22}\mathcal{Q}'\mathcal{Q}-\mathcal{Q}'^2)\sin^2\theta+(\mathcal{K}_{22}-1)\mathcal{Q}'^2\sin^4\theta\right]\rho\,d\rho+\frac{\mathcal{K}_{22}}{2}\,\mathcal{Q}^2+\frac{\mathcal{W}_+}{2}\sin^2\theta(1). \quad (19)$$

The minimization of the free energy with respect to the angle θ leads to the equation

$$\frac{d^2\theta}{d\rho^2}+\frac{1}{\rho}\,\frac{d\theta}{d\rho}+A\,\sin2\theta-B\,\sin4\theta=0, \quad (20)$$

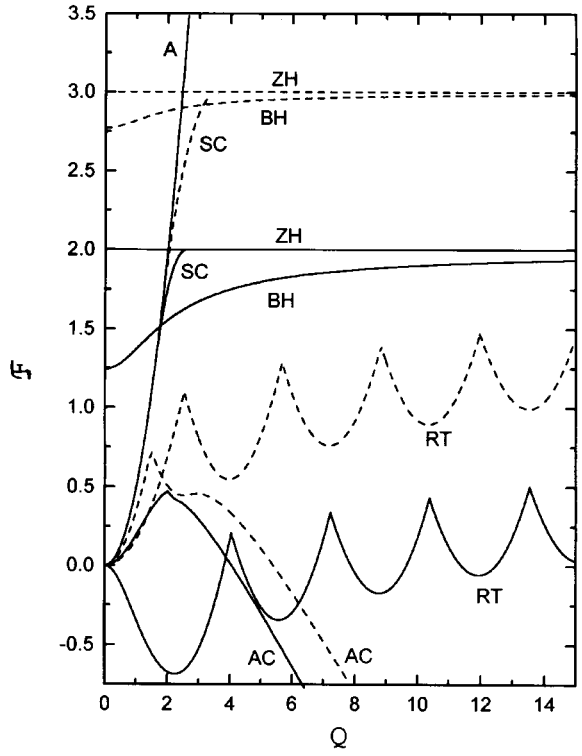

FIG. 4. Reduced free energy of different structures as a function of the reduced chirality parameter for $\mathcal{K}_{22}=1$, $\mathcal{K}_{24}=1$, $\mathcal{W}_\theta=4$, and two values of $\mathcal{W}_\phi$: 0 (full lines) and 2 (dotted lines).

where we have introduced the constants $A=[\mathcal{K}_{22}/(1+\mathcal{K}_{22})](2\mathcal{Q}\mathcal{Q}'-\mathcal{Q}'^2)$ and $B=[(1-\mathcal{K}_{22})/2(1+\mathcal{K}_{22})]\mathcal{Q}'^2$. The boundary condition is

$$\left(\frac{d\theta}{d\rho}+\frac{\mathcal{W}_+}{2(1+\mathcal{K}_{22})}\sin 2\theta\right)_{\rho=1}=0. \tag{21}$$

This equation is solved by the relaxation method for ordinary differential equations. As in the BH case, the K_{24} energy term has no influence on the simple conical structure. The nematic director and free energy do not depend on each anchoring strength separately, but only on their sum $\mathcal{W}_+$.

The relation between the actual and natural inverse pitch is different from that in the BH case. For $\mathcal{K}_{22}>1$ we get $\mathcal{Q}'>\mathcal{Q}$, while for $\mathcal{K}_{22}<1$ the opposite is the case. For equal elastic constants the inverse pitches are equal. For fixed $\mathcal{W}_+$ we get three different structures for different values of $\mathcal{Q}$. For $\mathcal{Q}\leqslant\mathcal{Q}_1$ the axial structure is stable; conical structure persists between $\mathcal{Q}_1$ and $\mathcal{Q}_2$; above $\mathcal{Q}_2$ we have the z helical structure. The bottom limit $\mathcal{Q}_1$ and the upper limit $\mathcal{Q}_2$ of the SC structure are increasing functions of $\mathcal{W}_+$. Both transitions at $\mathcal{Q}_1$ and $\mathcal{Q}_2$ are continuous. Of course, A and ZH structures can be viewed as limiting cases of the SC structure. Unlike the BC structure, the SC structure converges into the ZH structure at finite chirality parameters.

The problem with this approximation for the conical structure is that for common values of physical parameters its free energy is always higher than the free energy of the radially twisted structure (Fig. 4). Therefore we introduce two further modifications of this simple model with the aim of reducing the free energy and making the conical structure stable in a part of the calculated phase diagram.

In the first model, which we call bipolar conical structure, there is an additional deformation of the nematic director in the (x,y) plane. In the second modification we neglect this deformation, but consider the dependence of the conical tilt angle on both the radius and the azimuthal angle. The mirror symmetry with respect to local x' and y' axes of the tilt angle is therefore broken, which we stress by introducing the term asymmetric conical structure.

We must emphasize the similarity of the twist character of the yz twisted structure and all our conical models. Although it may seem at first glance that for conical structures there is only a twist around the z axis, in fact, there is also a local twist around the rotating y' axis because of the tilt of the nematic director out of the (x,y) plane. Let us now describe in more detail the two modified conical structures (Secs. III G and III H).

G. Bipolar conical structure

The nematic director in this case is a combination of the BH and SC structures: $\vec{n}=\sin\theta(\rho)\cos\psi(\rho,\phi')\vec{e}_\rho+\sin\theta(\rho)\sin\psi(\rho,\phi')\vec{e}_\phi+\cos\theta(\rho)\vec{e}_z$, where again $\phi'=\phi-q'z$. We require the symmetry of the nematic director with the respect to both the x' and y' axes in the rotating coordinate frame, as in the case of the BH structure. The tilt angle depends only on the radius, as in the simple conical model.

Minimization of the free energy with respect to variables θ and ψ yields a coupled system of an ordinary and a partial differential equation, which is solved numerically, and then the free energy is calculated. The free energy is minimized with respect to the twist parameter $\mathcal{Q}'$. It turns out again (as for the BH structure) that the actual inverse pitch can be approximated by the natural one. Keeping $\mathcal{W}_\phi$ and $\mathcal{W}_\theta$ fixed and increasing the inverse pitch we get three structures, as in the case of the simple conical model. Instead of the phase sequence A→SC→ZH, we have now the sequence A→BC→BH. The BC free energy is very near the SC value in almost all cases, except near the BC→BH transition. It is still higher than the RT free energy. Also the boundary values of the chiralities $\mathcal{Q}_1$ and $\mathcal{Q}_2$, where continuous transitions happen, are almost the same as in the simple conic model (for the same anchoring strengths). The main difference is that here we have a transition to a bipolar helical structure instead of to a z helical structure. But at the point $\mathcal{Q}_2$ where this happens, the BH structure is almost equal to the helical limit ZH structure. So the BC modification of the simple conic model does not bring any qualitative difference in the predicted behavior of the liquid crystal.

H. Asymmetric conical structure

Here the ansatz for the nematic director is the same as in the simple conical model, except that we allow the angular dependence of the tilt angle as well as the radial dependence $\vec{n}=\sin\theta(\rho,\phi')\cos(q'z)\vec{e}_x+\sin\theta(\rho,\phi')\sin(q'z)\vec{e}_y+\cos\theta(\rho,\phi')\vec{e}_z$. As before, we use the notation $\phi'=\phi-q'z$. We consider the case of equal elastic constants K_{ii}, but we allow the variation of K_{24}. We require no symmetry of the azimuthal dependence of the tilt angle. This has significant consequences on the equilibrium nematic director field, re-

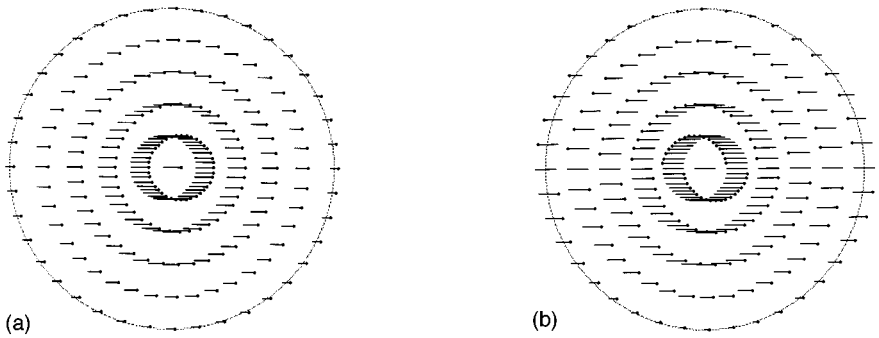

FIG. 5. Comparison of the nematic director field of a simple conical (left) and an asymmetric conical (right) structure in the (x',y') plane. Heads on the nails indicate the inclination in the negative z direction. The parameters are $\mathcal{K}_{24}=1$, $\mathcal{W}_\phi=\mathcal{W}_\theta=3$, and $\mathcal{Q}=2.2$.

sulting free energy, and the stability of the conical structure. The expression for the bulk free-energy density is

$$f_V=\frac{K}{2R^2}\left[\left(\frac{\partial\theta}{\partial\rho}\right)^2+\left(\frac{1}{\rho^2}+\mathcal{Q}'^2\right)\left(\frac{\partial\theta}{\partial\phi'}\right)^2 +2(\mathcal{Q}'\sin^2\theta-\mathcal{Q})\frac{\partial\theta}{\partial\rho}\sin\phi'+\frac{2}{\rho}(\mathcal{Q}'\sin^2\theta-\mathcal{Q}) \times\frac{\partial\theta}{\partial\phi'}\cos\phi'+(\mathcal{Q}'^2-2\mathcal{Q}\mathcal{Q}')\sin^2\theta+\mathcal{Q}^2\right] \quad (22)$$

and the surface free energy density is equal to

$$f_S=\frac{K}{2R}\left[(\mathcal{W}_\phi\sin^2\phi'+\mathcal{W}_\theta\cos^2\phi')\sin^2\theta -\mathcal{K}_{24}\mathcal{Q}'\left(\frac{\partial\theta}{\partial\phi'}\cos\phi'-\frac{1}{2}\sin2\theta\sin\phi'\right)\right]. \quad (23)$$

The resulting Euler-Lagrange differential equation is

$$\frac{\partial^2\theta}{\partial\rho^2}+\frac{1}{\rho}\frac{\partial\theta}{\partial\rho}+\left(\frac{1}{\rho^2}+\mathcal{Q}'^2\right)\frac{\partial^2\theta}{\partial\phi'^2} +\frac{1}{2}(2\mathcal{Q}\mathcal{Q}'-\mathcal{Q}'^2)\sin2\theta=0, \quad (24)$$

with the boundary condition

$$\left[\frac{\partial\theta}{\partial\rho}+(1-\mathcal{K}_{24})\mathcal{Q}'\sin^2\theta\sin\phi'-\mathcal{Q}\sin\phi' +\frac{1}{2}(\mathcal{W}_\phi\sin^2\phi'+\mathcal{W}_\theta\cos^2\phi')\sin2\theta\right]_{\rho=1}=0. \quad (25)$$

This differential equation is solved numerically by the relaxation method. It turns out that for many physical parameters the sinusoidal dependence of the conic angle is quite a good approximation: $\theta(\rho,\phi')\approx f(\rho)+g(\rho)\sin\phi'$, where f is a decreasing function of the radius, while g increases with the radius and $g(0)=0$. This contradicts the simple conical model (Fig. 5).

For low chiralities $f=0$, g is approximately linear, and the nematic structure is similar to the YZ structure. For chiralities above some critical value the tilt angle at the cylinder axis is different from zero and the twist of the nematic director about the z axis becomes appreciable. For still higher chiralities we get $f(\rho)\equiv\pi/2$ and the structure becomes more similar to planar structures. The chirality about the z axis rises and in the high-chirality limit it approaches the natural value (if $\mathcal{K}_{24}>0$). The $\mathcal{K}_{24}$ energy term is very important in the asymmetric conical structure. In the high-chirality limit it makes its energy even highly negative, thus much lower than the RT and YZ free energies. It also makes the structure planarlike, although not completely planar. Only in the case $\mathcal{K}_{24}=0$ does the AC structure approach the y twisted structure in the high-chirality limit. With increas-

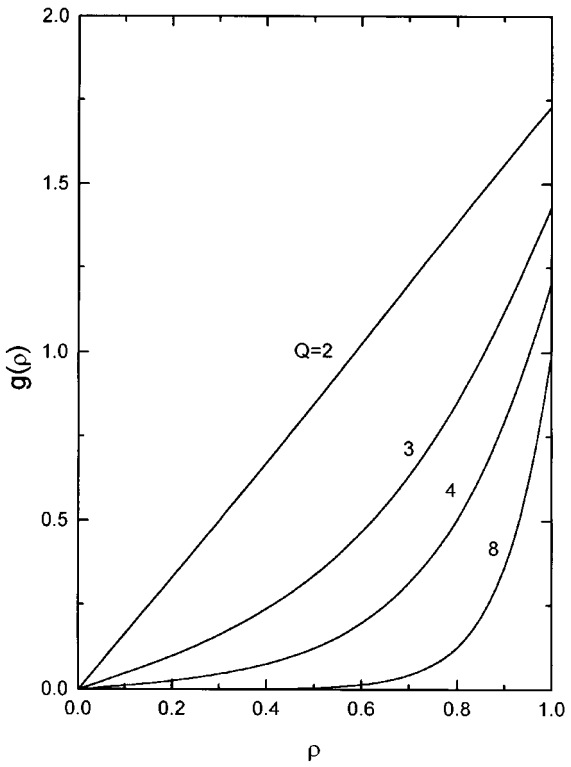

FIG. 6. Amplitude g of the sinusoidal modulation of the conic angle in the AC structure as a function of the reduced radius [in the approximation $\theta(\rho,\phi')\approx\pi/2+g(\rho)\sin\phi'$]. The parameters are $\mathcal{W}_\theta=4$, $\mathcal{W}_\phi=2$, $\mathcal{K}_{24}=1$, and different values of $\mathcal{Q}$.

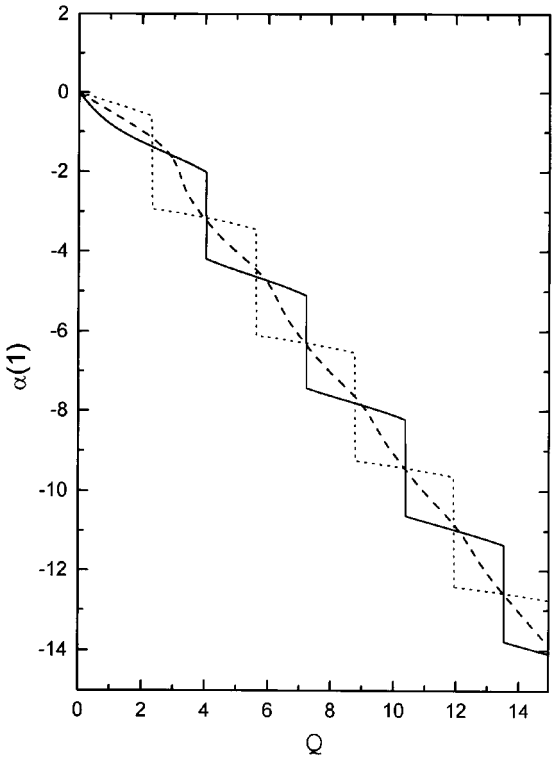

FIG. 7. Twist angle of the RT structure at the cylinder boundary as a function of the reduced chirality for $\mathcal{K}_{22}=1$, $\mathcal{W}_{\phi}=0$, and different values of $\mathcal{K}_{24}$: 1 (solid lines), 0 (dashed lines), and -2 (dotted lines).

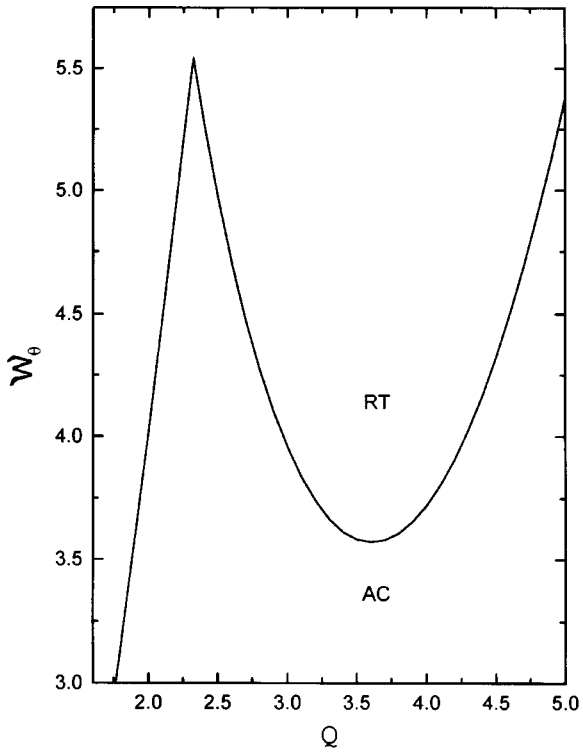

FIG. 8. RT-AC phase diagram in the $(\mathcal{Q},\mathcal{W}_{\theta})$ plane for $\mathcal{K}_{24}=1$ and $\mathcal{W}_{\phi}=3$. Both coordinates of the diagram are reduced (dimensionless).

ing chirality towards very high values the function g becomes more and more singular: it is almost zero inside, but it sharply increases to a finite value at the cylinder boundary. Some examples of this function are shown in Fig. 6. This indicates the possible formation of defects on the cylindrical boundary in the high-chirality limit. For low chiralities the chirality $\mathcal{Q}'$ is smaller than natural chirality $\mathcal{Q}$, but for higher chiralities their difference vanishes.

A more detailed description of this structure will be given elsewhere, together with a more general model of the conical structure, where also a deformation of the nematic director field projection within the xy plane is included. This requires the numerical solution of the system of two partial differential equations, so it takes a lot of computational time to cover enough of the parameter space. We have already succeeded in using the more general model in some narrow range of parameters, (especially for very low chiralities) and we have found that the resulting free energies are very similar to the energies of the simpler asymmetric conical structure presented here.

I. Radially twisted structure

The nematic director of the radially twisted structure, generally known as the ''double twisted structure'' [6,16], can be written as $\vec{n}=\sin\alpha(\rho)\vec{e}_{\phi}+\cos\alpha(\rho)\vec{e}_{z}$, where the twist angle α between the cylinder axis and nematic director depends only on the radius ρ. Here the nematic director rotates around any radial axis, i.e., any axis perpendicular to the cylinder axis.

The double twist character of this director field is pronounced at the cylinder axis and gradually fades away for increasing radius ρ. This structure also plays an important role in the theory of blue phases [16–18]. The RT structure has already been described in [10] and also in many other articles [6], so we give just a brief description here. As in the asymmetric conical structure, the K_{24} term is significant. It acts in a way similar to surface anchoring, but contrary to anchoring it lowers the RT free energy and makes the RT phase stable in a part of the phase diagram. The importance of the K_{24} elastic constant has been appreciated recently and several experiments have been performed to determine its value [19–21]. The minimization of the Frank free energy leads to the ordinary differential equation for the twist angle, which is solved numerically. The solution for $\alpha(\rho)$ and the free energy depends strongly on $\mathcal{K}_{24}$. The dependences of the angle at the cylinder boundary $\alpha(1)$ and of the free energy on chirality $\mathcal{Q}$ for fixed saddle-splay elastic constant have some interesting properties. There is a qualitative difference between the case $\mathcal{K}_{24}<0.36$ and the case $\mathcal{K}_{24}>0.36$. In the former case the boundary twist angle is a continuous function of the inverse pitch, while in the latter case there are discontinuous jumps at particular values of $\mathcal{Q}$ (Fig. 7). These jumps are caused by the competition between the twist energy term and K_{24} term. The free energy as a function of $\mathcal{Q}$ has minima and maxima. Minima are always smooth, while for $\mathcal{K}_{24}>0.36$ the derivatives of the free energy with respect to $\mathcal{Q}$ at maxima are discontinuous. The free energy as a function of inverse pitch has a sawtooth shape. The period between the minima or maxima is approximately π.

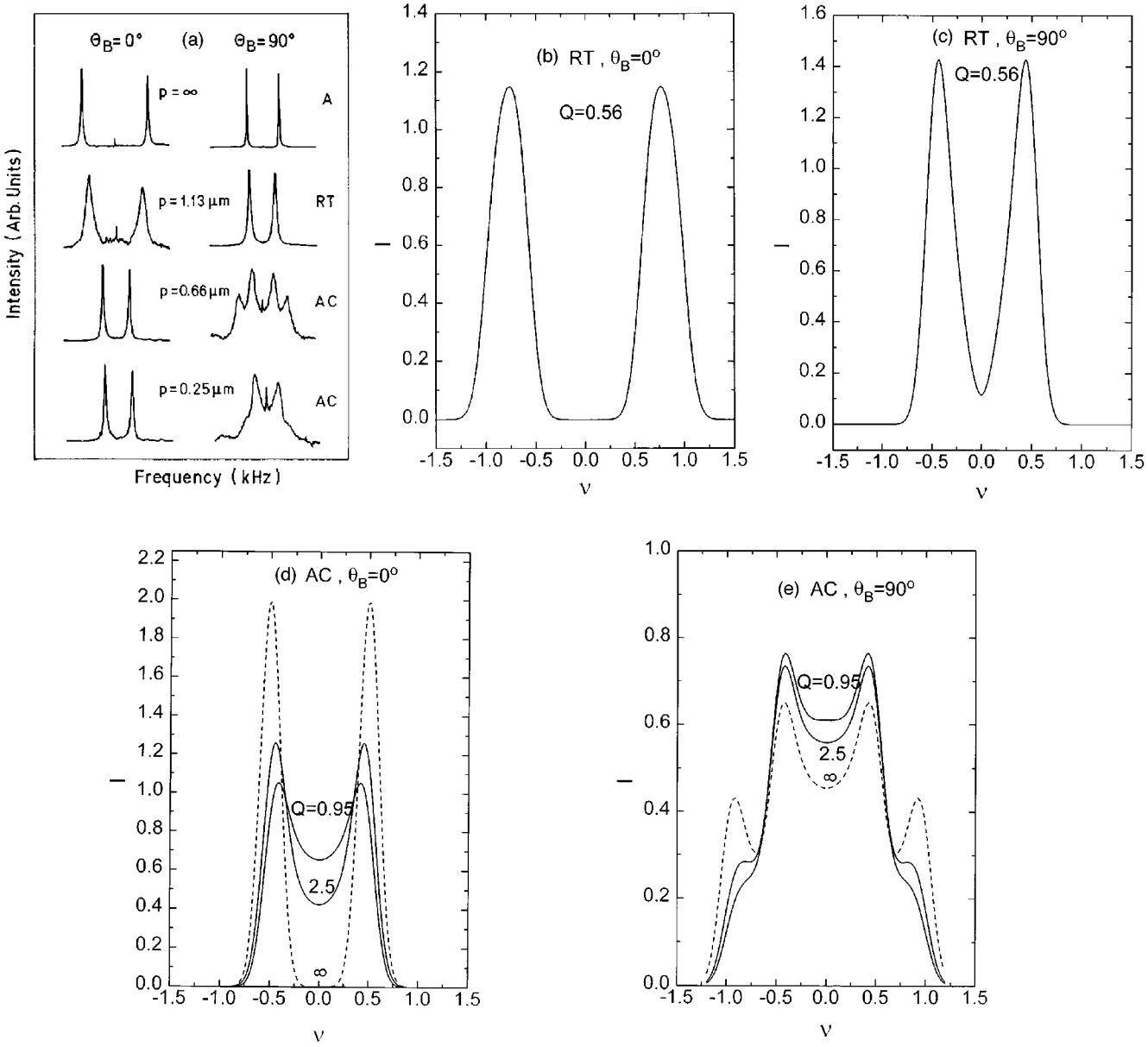

FIG. 9. Comparison between the (a) experimental NMR spectra from Ref. [10] and (b)–(e) calculated spectra for a magnetic field parallel ($\theta_B=0$) and normal ($\theta_B=90°$) to the cylinder axis for different pitches. Dashed lines in (d) and (e) indicate the spectra of limiting z helical structure. Frequencies and intensities in theoretical spectra are dimensionless. Intensities are normalized in a way to make the area under the curves equal to 1. For definition of the dimensionless frequency see the text.

IV. PHASE DIAGRAMS AND THE EXPLANATION OF EXPERIMENTS

We have found out that among all the structures that we considered, only radially twisted and asymmetric conical appear in phase diagrams, except at zero chirality, where we have axial structure. The RT structure is stable at low chiralities, while the AC structure is stable for high chiralities. All other structures have higher free energies.

The simplest representation of the phase diagram is obtained by fixing the values of elastic constants and one of the anchoring strengths. Then the phase diagram can be shown in two-dimensional space, where one coordinate is the inverse pitch and the other is the variable anchoring strength. Even in this case the computation of the phase diagram takes a lot of time. Therefore we present here only one calculated example of the phase diagram for chosen parameters $\mathcal{K}_{22}=\mathcal{K}_{24}=1$ and $\mathcal{W}_\phi=3$ (Fig. 8) and focus our attention on a discussion of available experimental data.

In an experiment by Ondris-Crawford *et al.* the nonchiral nematic liquid crystal 5CB-αd_2 (deuterated 4′-pentyl-4-cyanobiphenyl) with chiral agents CB15 and CE2 (EM Industries) was used [10]. The chirality was controlled by variable concentrations of chiral agents. The mixture was filled into the cavities ($R=0.1$ μm) of Anopore membranes, which are supposed to give planar anchoring conditions. The director field inside the cavities was observed by deuterium NMR with the magnetic field parallel and normal to the cylindrical axis. Increasing the chirality of the mixture, the NMR spectra indicate a transition from a definitely nonplanar structure to a roughly planar structure at

a pitch value of about 0.7 μm. The suggested low-chirality structure was radially twisted, while the high-chirality structure was supposed to be bipolar helical with a planar director field. Conical structures were not considered. Comparing the free energies, we calculated phase diagrams with BH and RT structures. After comparing BH-RT phase diagrams for different values of the saddle-splay elastic constant K_{24} in the case of equal bulk elastic constants and degenerate planar anchoring, the value $\mathcal{K}_{24}$ was predicted to be 0.1 ± 0.1. The anchoring strength was estimated also: $\mathcal{W}_\theta\approx0.15$. Both the value of the saddle-splay elastic constant and of the polar anchoring strength are an order of magnitude smaller than the ones predicted by several other experiments.

Here we have shown that the high-chirality structure should be asymmetric conical instead of bipolar helical form. From the nematic director field the NMR spectra for different structures were calculated, taking the half-width of spectral lines to be 0.1 by making a convolution with the Gaussian curve. The value 0.1 is taken in units of normalized frequency ν, where the two peaks in NMR spectra of axial structure with the magnetic field parallel to cylinder axis are at the positions $\nu=\pm1$. A comparison of the calculated and measured spectra (Fig. 9) indicates the following. First, the low-chirality structure is really RT and we can also make an estimation $\mathcal{K}_{24}-\mathcal{W}_\phi\approx1$. Thus the value of $\mathcal{K}_{24}$ must be at least 1. From various experimental data the actual value seems to be $1<\mathcal{K}_{24}<2$. Thus we investigated this interval and by a comparison of RT and AC free energies we obtained the values of polar anchoring strength $0<\mathcal{W}_\theta<1$. On the basis of this argument the $\mathcal{K}_{24}$ value seems to be closer to 2 than to 1. We estimated the values of the parameters $\mathcal{K}_{24}\approx1.5\pm0.5$, $\mathcal{W}_\theta\approx0.5\pm0.5$, and $\mathcal{W}_\phi\approx0.5\pm0.5$. Taking a typical value of bulk elastic constants $K_{ii}\approx5\times10^{-12}$ J/m, we obtain $K_{24}\approx(7.5\pm2.5)\times10^{-12}$ J/m and $W_\theta, W_\phi\approx(2.5\pm2.5)\times10^{-5}$ J/m^2. The agreement between the spectra for the RT structure is very good [Figs. 9(a)–9(c)]. Agreement between the calculated and experimental spectra for the AC structure is somewhat worse [Figs. 9(a), 9(d), and 9(e)], but nevertheless all important features of the spectra are qualitatively explained. The asymmetric conical structure should be more planarlike, i.e., the calculated spectra should be closer to z helical spectra [dashed lines in Figs. 9(d) and 9(e)]. This inconsistency may appear because we do not treat the most general model, where we would also have a deformation of the nematic director field within the (x,y) plane. In theoretical spectra [Figs. 9(b)–9(e)], the chiralities correspond to experimental pitches [Fig. 9(a)] $p=1.13$ μm $\rightarrow\mathcal{Q}=0.56$, $p=0.66$ μm$\rightarrow\mathcal{Q}=0.95$, and $p=0.25$ μm$\rightarrow\mathcal{Q}=2.5$.

In another experiment, performed by Schmiedel and coworkers [15,22], optical measurements and ^{2}H and ^{13}C NMR studies were performed on chiral nematic liquid crystals adsorbed in Anopore membranes with cylindrical pores of radius 0.1 μm. Three types of compounds were used: pure cholesteryl undecyl carbonate (ChUC), a nematic mixture M5 with chiral dopant ChUC, and ferroelectric p-decyloxy-bezylidene-p-amino-2-methyl-butyl-cinnamate (DOBAMBC). The pitch was varied by changing the temperature or the concentration of ChUC in the M5 mixture. The anchoring condition was supposed to be tangential with the preferred z axis direction. The angular dependence of the NMR spectra was obtained by rotating the NMR glass tube around its axis, where the pore axes were uniformly directed normal to the rotation axis. Simulation of the angular dependence of NMR spectra leads to the estimation of the tilt angle distribution of the molecules with respect to the z axis. They also found the optical activity in their samples for a wide range of chiralities. The polarization of the light incident in the cylinder axis direction rotates around that axis, which is not the case for the RT structure. They suggested the structure to be simple conical. On the basis of the NMR spectra for different directions of the magnetic field they calculated the distribution of conical angle. In Fig. 10 two of their distributions [(a) and (b)] are compared to the ones obtained for the asymmetric conical structure [(c)]. Unfortunately, the authors [15] do not specify the chiralities used in the corresponding experiments. Therefore, we just take a set of parameters that yield qualitatively similar distributions. We also calculated the angular distribution densities for the angles between the nematic director and the z axis for other structures considered, but they are all qualitatively different from the experimental functions.

As we have seen, no planar structures appear to be stable for degenerate anchoring or z anchoring. In the high-chirality case the stable asymmetric conical structure exhibits a ''quasiplanar'' behavior. But it should be stressed that it is stable only because of the nonzero K_{24} elastic energy term. For $K_{24}=0$ the structure with rotation of the nematic director around the axis, perpendicular to the cylinder axis, is more stable than the structure with rotation of the nematic director around the cylinder axis. If we generalize the form of the AC director field to include the deformation of its projection in the (x,y) plane, the new structure is expected to have features of both asymmetric conical and bipolar helical structures. We have shown that upon increasing chirality the nematic director field of the planar BH structure is more and more aligned. But in the strong anchoring limit the strong deformation of nematic director fields at particular points at the cylinder boundary (which results in defects) persists even for high chiralities. On the other hand, the AC structure is more and more planar in the high-chirality limit. Therefore, it is expected that the generalized AC structure is very similar to the BH structure for high chiralities. Thus, in the case of very strong anchoring and high chiralities, the study of defects in the chiral planar bipolar structures by Bezič and Zumer [8] may be of interest. In [8] topological features were studied, but not the detailed nematic director fields and free energies. In addition, it should be stressed that the stability of planar structures could be enhanced if the preferred anchoring direction is $\vec{e}_\phi$ (concentric planar anchoring) instead of $\vec{e}_z$.

V. CONCLUSION

We have reviewed various model structures of chiral nematic liquid crystals confined to cylindrical cavities with planar anchoring conditions. We have calculated the nematic director fields and the resulting free energies of the axial, z helical and y helical structures, the bipolar helical, yz twisted structure, three models of conical structure, and the radially twisted structure in the case of equal bend and splay elastic constants. The K_{13} energy term has been neglected, but the K_{24} term has been taken into account. The saddle-splay term

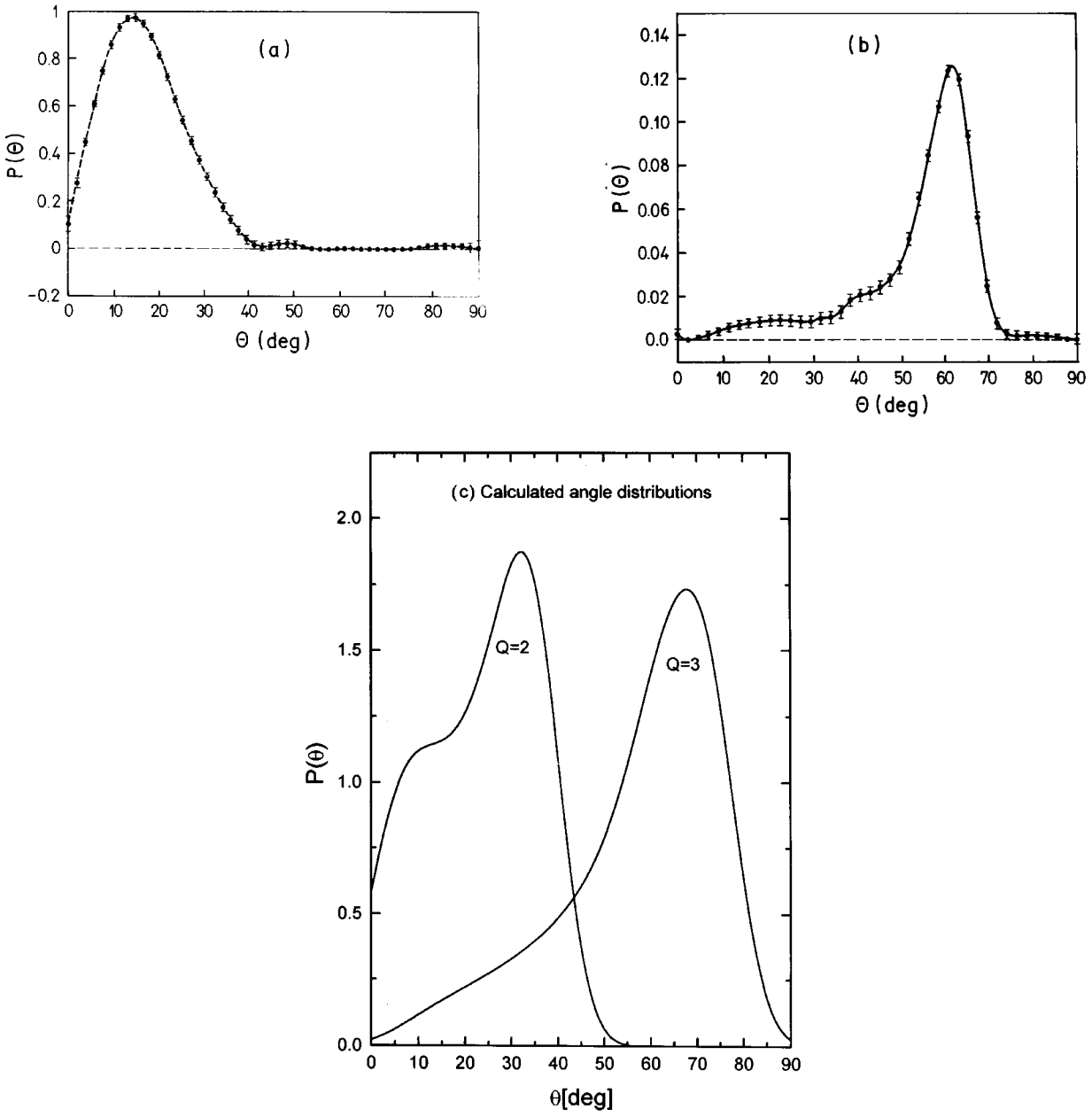

FIG. 10. Two model experimental distribution densities of a conical angle (a) and (b) from Ref. [15] for two different chiralities and two theoretical distributions (c) for $Q=2$ and 3, corresponding to the model AC structure. The parameters for the theoretical distributions are $\mathcal{K}_{24}=0$, $\mathcal{W}_{\phi}=\mathcal{W}_{\theta}=3$.

significantly affects the asymmetric conical and radially twisted structures and it plays an important role in phase diagrams. The radially twisted and asymmetric conical structures are the only ones that appear in the main regions of the phase diagram. The former structure is stable for lower chiralities and the latter for higher chiralities. We have also found that in general the pitch of the confined system is different from the bulk value and depends on the ratios between the bulk elastic constants.

We have compared our results with some available experimental data and found good agreement. We have estimated the value of saddle-splay elastic constant of nematic 5CB doped with CB15 and CE2: $K_{24}/K \approx 1.5 \pm 0.5$.

A number of generalizations could be included in our calculations, which we expect would induce minor changes in our stability phase diagrams, but would make procedures much more complex [24–26]. Therefore a more general form of the nematic director field is left for future considerations. We believe that it can lead to some mixed structures, for instance, the RT structure, modulated by the conical structure in the core of the cylinder. This possibility is indicated by the experiments of Lequex and Kleman [6] and by Kitzerow *et al.* [23], who observed the helical instability of the doubly twisted structure.

ACKNOWLEDGMENTS

This research was funded in part by the Ministry of Science and Technology of Slovenia under Project No. J1-7067 and by the European Commission under Project No. PECO ERBCIPDCT940602.

[1] P. P. Crooker, Liq. Cryst. **5**, 75 (1989), and references therein.
[2] J. W. Doane, *Liquid Crystals: Applications and Uses*, edited by B. Bahadur (World Scientific, Teaneck, NJ, 1990).
[3] Anotec Separations, 226 East 54th Street, New York, NY 10022.
[4] G. P. Crawford, L. M. Steele, R. J. Ondris-Crawford, G. S. Iannachione, C. J. Yeager, J. W. Doane, and D. Finotello, J. Chem. Phys. **96**, 7788 (1992).
[5] P. E. Cladis, A. E. White, and W. F. Brinkman, J. Phys. (Paris) **40**, 325 (1979).
[6] F. Lequex and M. Kleman, J. Phys. (Paris) **49**, 845 (1988).
[7] J. Bezič and S. Žumer, Liq. Cryst. **11**, 593 (1992).
[8] J. Bezič and S. Žumer, Liq. Cryst. **14**, 1695 (1993).
[9] R. J. Ondris-Crawford, G. P. Crawford, S. Žumer, and J. W. Doane, Phys. Rev. Lett. **70**, 194 (1993).
[10] R. J. Ondris-Crawford, M. Ambrozic, J. W. Doane, and S. Žumer, Phys. Rev. E **50**, 4773 (1994).
[11] G. Chidichimo, Z. Yaniv, N. A. Vaz, and J. W. Doane, Phys. Rev. A **25**, 1077 (1982).
[12] F. C. Frank, Discuss. Faraday Soc. **25**, 19 (1985).
[13] B. Jerome, Rep. Prog. Phys. **54**, 391 (1991).
[14] A. Kilian and A. Sonnet, Z. Naturforsch. Teil A **50**, 991 (1995).
[15] H. Schmiedel, R. Stannarius, G. Feller, and CH. Cramer, Liq. Cryst. **17**, 323 (1994).
[16] E. Dubois-Violette and B. Pansu, Mol. Cryst. Liq. Cryst. **165**, 151 (1988).
[17] R. M. Hornreich and S. Strikman, Phys. Rev. A **38**, 4843 (1988).
[18] R. M. Hornreich and S. Strikman, Phys. Rev. A **41**, 1978 (1990).
[19] D. W. Allender, G. W. Crawford, and J. W. Doane, Phys. Rev. Lett. **67**, 1442 (1991).
[20] G. P. Crawford, D. W. Allender, and J. W. Doane, Phys. Rev. A **45**, 8693 (1992).
[21] R. D. Polak, G. P. Crawford, B. C. Kostival, J. W. Doane, and S. Žumer, Phys. Rev. E **49**, 978 (1994).
[22] Ch. Cramer, H. Schmiedel, and G. Feller (unpublished).
[23] H. S. Kitzerow, B. Liu, F. Xu, and P. P. Crooker, Phys. Rev. E **54**, 568 (1996).
[24] V. M. Pergamenshchik, Phys. Rev. E **48**, 1254 (1993).
[25] V. M. Pergamenshchik, P. I. C. Teixeira, and T. J. Sluckin, Phys. Rev. E **48**, 1265 (1993).
[26] G. Barbero and A. Strigazzi, Liq. Cryst. **5**, 693 (1989).